Free Radical Research, October 2005; 39(10): 1027–1033

Spin trapping nitric oxide from neuronal nitric oxide synthase: A look at several iron–dithiocarbamate complexes

JOHN WEAVER[1,2,5], SUPATRA PORASUPHATANA[3], PEI TSAI[2,5], THEODORE BUDZICHOWSKI[1], & GERALD M. ROSEN[2,4,5]

[1]*Department of Chemistry, University of Maryland Baltimore County, Baltimore MD 21250, USA,* [2]*Department of Pharmaceutical Sciences, University of Maryland School of Pharmacy, Baltimore MD 21201, USA,* [3]*Faculty of Pharmaceutical Science, Department of Toxicology, Khon Kaen University, Khon Kaen 40002, Thailand,* [4]*Medical Biotechnology Center, University of Maryland Biotechnology Institute, Baltimore MD 21201, USA, and* [5]*Center for Low Frequency EPR Imaging for* In Vivo *Physiology, University of Maryland, Baltimore MD 21201, USA*

Accepted by Dr T. Finkel

(Received 16 June 2005; In final form 29 June 2005)

Abstract

The free radical, nitric oxide (·NO), is responsible for a myriad of physiological functions. The ability to verify and study ·NO *in vivo* is required to provide insight into the events taking place upon its generation and in particular the flux of ·NO at relevant cellular sites. With this in mind, several iron-chelates ($Fe^{2+}(L)_2$) have been developed, which have provided a useful tool for the study and identification of ·NO through spin-trapping and electron paramagnetic resonance (EPR) spectroscopy. However, the effectiveness of ·NO detection is dependent on the $Fe^{2+}(L)_2$ complex. The development of more efficient and stable $Fe^{2+}(L)_2$ chelates may help to better understand the role of ·NO *in vivo*. In this paper, we present data comparing several proline derived iron–dithiocarbamate complexes with the more commonly used spin traps for ·NO, Fe^{2+}-di(*N*-methyl-D-glutamine-dithiocarbamate) ($Fe^{2+}(MGD)_2$) and Fe^{2+}-di(*N*-(dithiocarboxy)sarcosine) ($Fe^{2+}(DTCS)_2$). We evaluate the apparent rate constant (k_{app}) for the reaction of ·NO with these $Fe^{2+}(L)_2$ complexes and the stability of the corresponding $Fe^{2+}(NO)(L)_2$ in presence of NOS I.

Keywords: *Nitric oxide, spin trapping, EPR, nitric oxide synthase*

Abbreviations: EPR, electron paramagnetic resonance; NOS, nitric oxide synthase; $Fe^{2+}(DETC)_2$, Fe^{2+}-di(*N,N*-diethyldithiocarbamate); $Fe^{2+}(MGD)_2$, Fe^{2+}-di(*N*-methyl-D-glutaminedithiocarbamate); $Fe^{2+}(DTCS)_2$, Fe^{2+}-di(*N*-(dithiocarboxy)sarcosine); $Fe^{2+}(DTCP)_2$, Fe^{2+}-di(*N*-(dithiocarboxy)-L-proline); $Fe^{2+}(DTCHP)_2$, Fe^{2+}-di(*N*-(dithiocarboxy)-*trans*-4-hydroxy-L-proline); $Fe^{2+}(MSD)_2$, Fe^{2+}-di(*N*-(dithiocarboxy)-*N*-methyl-L-serine); $Hb(Fe^{2+})O_2$, oxyhemoglobin

Introduction

A new era of free radical research was introduced with the discovery that the free radical, nitric oxide (·NO), was responsible for the physiological activity attributed to the endothelium derived relaxation factor (EDRF) [1–4], and subsequent discovery that the enzyme, nitric oxide synthase (NOS), catalyzed the oxidative metabolism of L-arginine to L-citrulline and ·NO [5–7]. There are three distinct isoforms of NOS: The constitutively expressed neuronal NOS (nNOS or NOS I) and endothelial NOS (eNOS or NOS III), and the inducible NOS (iNOS or NOS II) [8]. The ·NO, generated from these three isoforms, has been shown to regulate many physiological functions such as vascular tone, host immune response and neurotransmission [9].

Among the many methods known to detect ·NO [10] spin trapping/EPR spectroscopy has proven to be

Correspondence: J. Weaver, Department of Pharmaceutical Sciences, University of Maryland School of Pharmacy, 725 W. Lombard Street S332, Baltimore MD 21201, USA. Tel: 410 706 7420. Fax: 410 706 8184. E-mail: jweav001@umaryland.edu

ISSN 1071-5762 print/ISSN 1029-2470 online © 2005 Taylor & Francis
DOI: 10.1080/10715760500231885

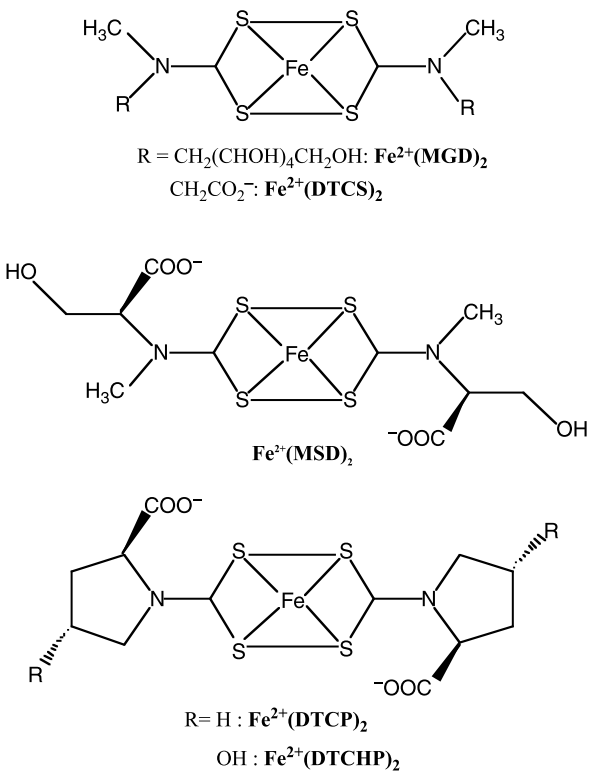

Figure 1. Fe^{2+}—chelates used as spin traps for ·NO.

a reliable technique for the identification of this free radical, especially in animal models. One class of spin traps for ·NO is nitronyl nitroxides [11,12], whose susceptibility to bioreduction has fostered the synthesis of a family of dendrimer-containing nitronyl nitroxides, which exhibit enhanced resistance toward reduction [13]. A second family of spin traps for ·NO includes iron-chelates ($Fe^{2+}(L)_2$) such as Fe^{2+}-di(*N*,*N*-diethyldithiocarbamate) ($Fe^{2+}(DETC)_2$) [14–16], Fe^{2+}-di(*N*-methyl-D-glutamine-dithiocarbamate) ($Fe^{2+}(MGD)_2$) [17,18], and Fe^{2+}-di(*N*-(dithiocarboxy)sarcosine) ($Fe^{2+}(DTCS)_2$) [19–21] (Figure 1). The reaction between ·NO and $Fe^{2+}(L)_2$ results in a Fe^{2+}-nitrosyl complex, ($Fe^{2+}(NO)(L)_2$), in which the ·NO has a coordination bond with iron (Figure 2). These complexes, which exhibit a characteristic triplet EPR spectrum ($g = 2.040$, $A_N = 12.7$ G) at ambient temperature [20,22], appear to be relatively stable in biological milieu. This latter property enables *in vitro* and *in vivo* detection of ·NO [20,21,23], even though complications pertinent to specific $Fe^{2+}(L)_2$ complexes may restrict their use in some experimental designs [21].

In our continuous search for optimal $Fe^{2+}(L)_2$ complexes that will allow the *in vivo*, *in situ* detection of ·NO in real time using low-frequency EPR spectroscopy, several proline derived dithiocarbamate complexes have shown great promise as potential spin traps for ·NO (Figure 1) [24,25]. In this paper, we explore the utility of several iron–proline derived dithiocarbamate complexes to spin trap ·NO, determining the apparent rate constant (k_{app}) for this reaction and the stability of the corresponding $Fe^{2+}(NO)(L)_2$ chelates. The ability of the $Fe^{2+}(L)_2$ complexes to spin trap ·NO, generated from purified NOS I, was evaluated and compared to two of the most frequently used Fe^{2+}-dithiocarbamate chelates.

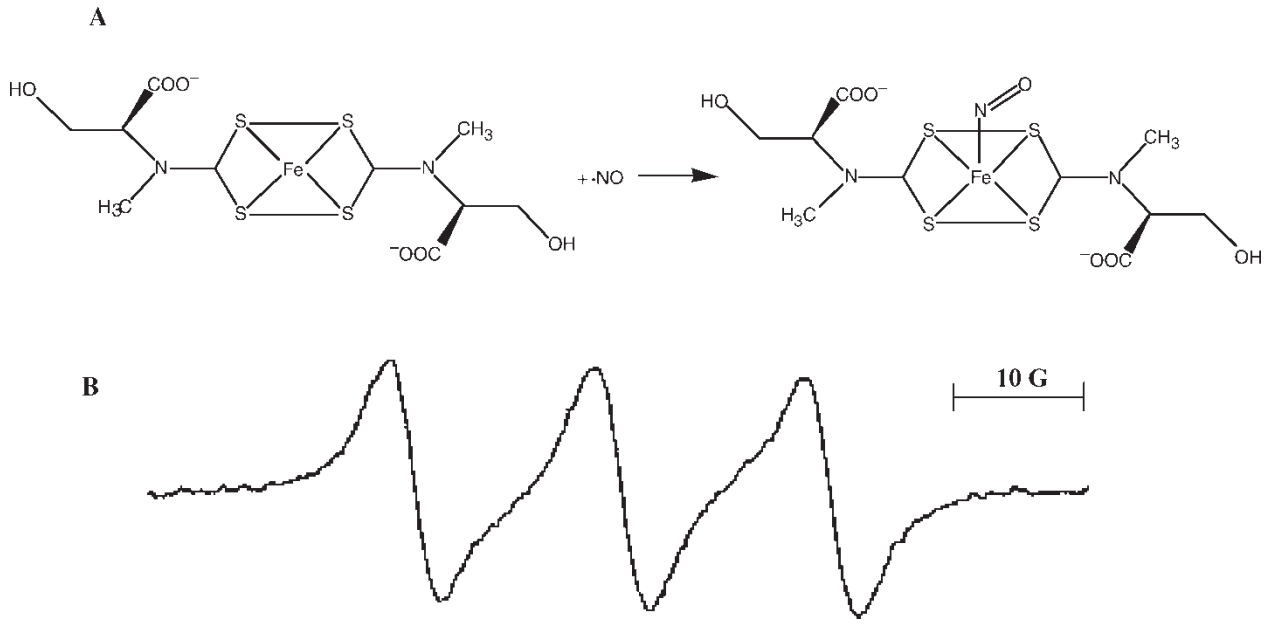

Figure 2. The reaction of $Fe^{2+}(L)_2$ and ·NO to form $Fe^{2+}(NO)(L)_2$. **(A)** The reaction of $Fe^{2+}(MSD)_2$ with ·NO to form $Fe^{2+}(NO)(MSD)_2$ is given along with **(B)** a typical EPR spectrum of $Fe^{2+}(NO)(MSD)_2$ from the reaction of $Fe^{2+}(MSD)_2$ (500 μM) with ·NO (50 μM) from a gaseous solution is shown. Receiver gain was 2×10^4.

Materials and methods

Reagents

Oxyhemoglobin ($Hb(Fe^{2+})O_2$), nicotinamide adenine dinucleotide phosphate (NADPH), calcium chloride ($CaCl_2$), calmodulin, L-proline, *trans*-4-hydroxy-L-proline and L-arginine were obtained from Sigma Chemical Company (St. Louis, MO). *N*-Methyl-L-serine was obtained from BACHEM Biosciences Inc. (King of Prussia, PA). Ferrous sulfate ($FeSO_4$) was purchased from Mallinckrodt (St. Louis, MO). Nitric oxide gas was purchased from Matheson Gas Products, Inc. (East Rutherford, NJ). Ammonium *N*-(dithiocarboxy)sarcosine (($NH_4)_2$DTCS) was synthesized according to the method described in Pou, et al. [21]. Sodium *N*-methyl-D-glucamine dithiocarbamate (NaMGD) was prepared as previously described [17]. All other chemicals were used as purchased without further purification. NOS I, expressed, isolated and purified, was provided by Dr. Linda Roman [26] (Department of Biochemistry at The University of Texas Health Science Center, San Antonio, TX). Purified NOS I was diluted to desired concentrations in Tris buffer (50 mM, pH 7.4 containing 100 mM NaCl).

Synthesis of Ammonium N-(dithiocarboxy)-L-proline ($(NH_4)_2$DTCP, Ammonium N-(dithiocarboxy)-trans-4-hydroxy-L-proline ($(NH_4)_2$DTCHP and Ammonium N-(dithiocarboxy)-N-methyl-L-serine ($(NH_4)_2$MSD.

The compounds ($(NH_4)_2$DTCP, ($(NH_4)_2$DTCHP and ($(NH_4)_2$MSD were synthesized according to methods described in Pou *et al.* and Nakagawa *et al.* with slight modifications [21,24]. To a solution of L-proline, *trans*-4-hydroxy-L-proline or N-methyl-L-serine in 30% ammonium hydroxide at 0°C was added carbon disulfide in absolute ethanol. The rate of addition was such that the temperature of the reaction did not exceed 10°C. The solution was stirred for 1 h as the temperature of the reaction was allowed to reach ambient conditions. The resulting solution was reduced to dryness *in vacuo*. And the remaining solids were recrystallized from ethanol for ($(NH_4)_2$-DTCP and from methanol for ($(NH_4)_2$DTCHP and ($(NH_4)_2$MSD.

Spin trapping/EPR spectroscopy

Spin trapping experiments were conducted by mixing all components described in each figure legend to a final volume of 0.3 ml. The reaction mixture was then transferred to a flat quartz cell and placed into the cavity of an EPR spectrometer (Varian Associates model E-109, Palo Alto, CA). EPR spectra were recorded at room temperature after the reaction was initiated. Instrument settings were as follows: Microwave power, 20 mW; modulation frequency, 100 kHz; modulation amplitude, 0.5 G; sweep time, 12.5 G/min; and response time, 0.5 s. The receiver gain is given in each figure legend.

Preparation of $Fe^{2+}(NO)(L)_2$

The concentration of $Fe^{2+}(L)_2$ was estimated based on the concentration of Fe^{2+}, since the salts above were added at five times molar excess. $Fe^{2+}(NO)(L)_2$ were prepared as described in literature [18,20,21,27]. Briefly, an equal volume of ($(NH_4)_2$DTCP, ($(NH_4)_2$DTCHP, ($(NH_4)_2$MSD, ($(NH_4)_2$DTCS, or NaMGD (100 mM, dissolved in deionized water under N_2), was mixed with $FeSO_4$ (20 mM, dissolved in deionized water under N_2) to form $Fe^{2+}(L)_2$ at the desired concentration. To this solution of $Fe^{2+}(L)_2$, ·NO gas (50 μM, final concentration, in an aqueous solution) was added to form $Fe^{2+}(NO)(L)_2$. The concentration of ·NO was estimated by reaction with $Hb(Fe^{2+})O_2$ using an extinction coefficient of $12\,mM^{-1}\,cm^{-1}$ at 576 nm [28]. EPR spectra were recorded at room temperature using instrument settings described above.

Determination of k_{app} for the reaction of ·NO and $Fe^{2+}(L)_2$

The k_{app} for the reaction of ·NO with $Fe^{2+}(L)_2$ was determined according to the method described in Pou et al. [21]. An aqueous solution of gaseous ·NO (20–30 μM, final concentration), prepared in an anaerobic phosphate buffer at pH 7.4, was mixed with freshly prepared $Fe^{2+}(L)_2$ (200 μM), prepared as described above, in the absence and presence of $Hb(Fe^{2+})O_2$ (0–30 μM, final concentration). The concentration of $Hb(Fe^{2+})O_2$ was determined as previously described [28]. Reactions were immediately added to a quartz flat cell and introduced into the EPR spectrometer. EPR spectra were recorded at room temperature.

Spin trapping of NOS I-generated ·NO Using $Fe^{2+}(L)_2$ Complexes

Spin trapping of NOS I generated ·NO by $Fe^{2+}(L)_2$ was conducted by mixing L-arginine (100 μM), NADPH (1 mM), $CaCl_2$ (2 mM), and calmodulin (100 U/ml) in phosphate buffer (50 mM, pH 7.4, 1 mM EGTA) at room temperature. To this mixture was added $Fe^{2+}(L)_2$ (800 μM) and the reaction was initiated by the addition of purified NOS I (300 nM) to a final volume of 0.3 ml. The resultant solution was then transferred into a quartz flat cell, which was fitted into the cavity of the EPR spectrometer. EPR spectra were recorded continuously at room temperature up to 1 h after the initiation of the reaction, determining the efficiency and stability of each

Table I. K_{app} and stability measurements for the spin trapping of ·NO by $Fe^{2+}(L)_2$.

Fe^{2+}-chelate	Rate constant ($\times 10^6\,M^{-1}s^{-1}$)[a]		Stability in a NOS I system
	Calculated	Literature	
$Fe^{2+}(DTCS)_2$	1.11 ± 0.44	1.71 ± 0.30 [21]	Unchanged[b]
$Fe^{2+}(MGD)_2$	1.28 ± 0.43	1.21 ± 0.53 [21]	Unchanged
$Fe^{2+}(DTCP)_2$	4.88 ± 0.36	110 ± 30 [25]	Unchanged
$Fe^{2+}(DTCHP)_2$	1.70 ± 0.77	–	half-life: 15.5 min
$Fe^{2+}(MSD)_2$	1.04 ± 0.29	–	Unchanged

[a]Rates are the average of three independent experiments, expressed as the means and standard deviations.
[b]The term "unchanged" refers to the fact that over 1 h, there was no decrease in the EPR spectral peak height of $Fe^{2+}(NO)(L)_2$.

$Fe^{2+}(NO)(L)_2$ complex in the presence of the competent NOS I.

Results

In the first set of experiments, ·NO (50 μM in an aqueous solution) was added to preformed $Fe^{2+}(L)_2$ (500 μM, prepared as described in Materials and Methods) in phosphate buffer (30 mM, pH 7.4). The resultant $Fe^{2+}(NO)(L)_2$ complexes exhibited characteristic EPR spectra, similar to those reported in literature [20,22,29]. For illustrative purposes the EPR spectrum of $Fe^{2+}(NO)(MSD)_2$ is shown in Figure 2. Reaction of $Fe^{2+}(DTCS)_2$, $Fe^{2+}(MGD)_2$,

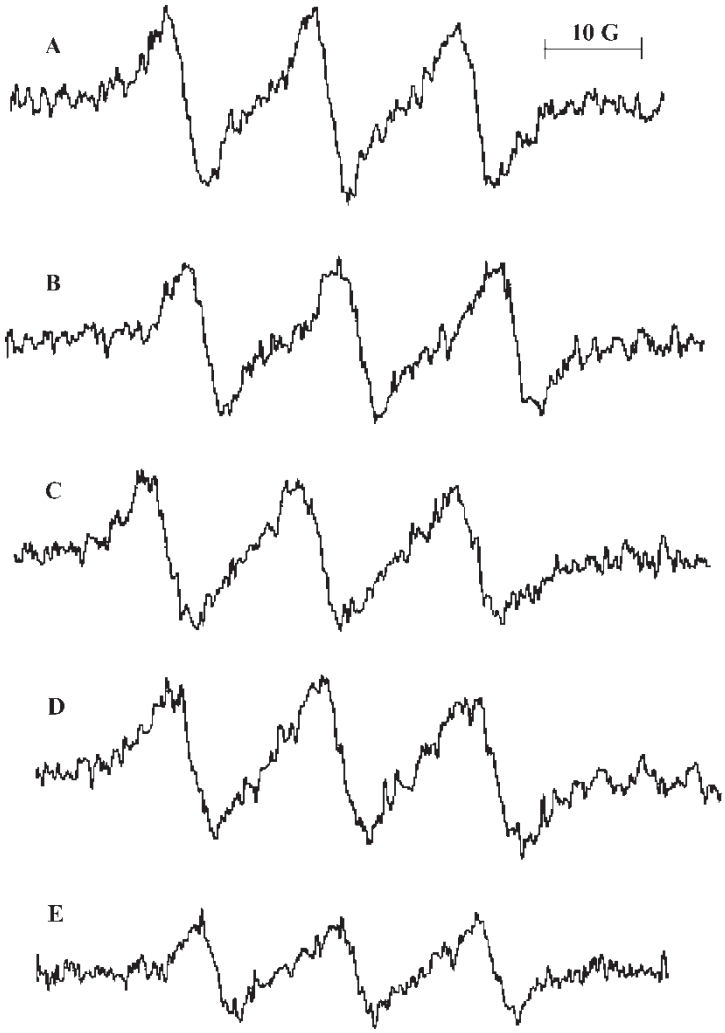

Figure 3. Typical EPR spectra of $Fe^{2+}(NO)(L)_2$ from the reaction of $Fe^{2+}(L)_2$ with NOS I-generated ·NO. The reaction system consisted of NOS I (300 nM), $CaCl_2$ (2 mM), calmodulin (100 U/ml), NADPH (1 mM), L-arginine (100 μM), chelate (4 mM) and $FeSO_4$ (800 μM) in phosphate buffer (50 mM, pH 7.4, 1 mM EGTA). **(A)** EPR spectrum of $Fe^{2+}(NO)(DTCS)_2$; **(B)** EPR spectrum of $Fe^{2+}(NO)(MSD)_2$; **(C)** EPR spectrum of $Fe^{2+}(NO)(DTCHP)_2$; **(D)** EPR spectrum of $Fe^{2+}(NO)(DTCP)_2$; **(E)** EPR spectrum of $Fe^{2+}(NO)(MGD)_2$. EPR spectra were recorded 10 min after addition of NOS I. Receiver gain was 10×10^4.

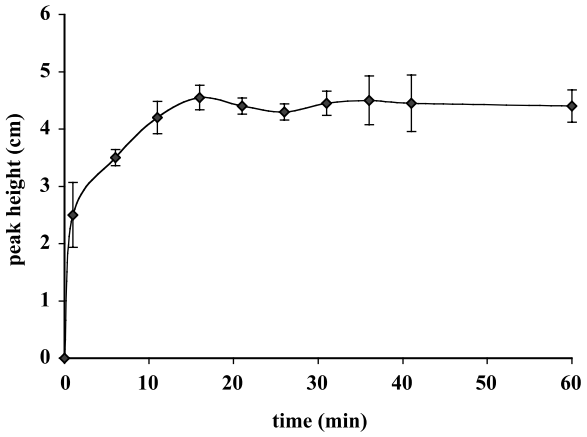

Figure 4. A representative plot of the increase in the first low-field peak of EPR spectrum of $Fe^{2+}(NO)(L)_2$ from the reaction of $Fe^{2+}(L)_2$ with NOS I generated ·NO over a hour time period. Similar data was obtained using the area under each EPR spectral line [36]. Data shown correspond to $Fe^{2+}(NO)(MSD)_2$. The spin traps, $Fe^{2+}(DTCS)_2$, $Fe^{2+}(MGD)_2$ and $Fe^{2+}(DTCP)_2$, gave similar data. Each point on the graph is the average of three independent experiments, expressed as the means and standard deviations.

$Fe^{2+}(DTCP)_2$, or $Fe^{2+}(DTCHP)_2$ with ·NO gave comparable EPR spectra. The addition of ·NO to solutions of $(NH_4)_2$DTCS, NaMGD, $(NH_4)_2$DTCP, $(NH_4)_2$DTCHP, $(NH_4)_2$MSD or $FeSO_4$ alone resulted in no EPR spectrum (data not shown), confirming that the iron-complexes were the spin traps for ·NO.

Next, the k_{app} for the reaction of ·NO with each of the spin traps was determined (Table I). The competitive kinetic model previously described was used for these experiments [21]. Briefly, an aqueous solution of ·NO was added to freshly prepared solutions of $Fe^{2+}(L)_2$ in the presence of varying concentrations of $Hb(Fe^{2+})O_2$, as the competitive inhibitor. $Hb(Fe^{2+})O_2$ is oxidized by ·NO with a rate constant of $3.7 \times 10^7\,M^{-1}s^{-1}$ at 25°C [30]. Using this method, the k_{app} for the reaction of $Fe^{2+}(DTCP)_2$, $Fe^{2+}(DTCHP)_2$ and $Fe^{2+}(MSD)_2$ with ·NO was found to be similar to those previously reported for $Fe^{2+}(DTCS)_2$ and $Fe^{2+}(MGD)_2$ (Table I). Like $Fe^{2+}(DTCS)_2$ and $Fe^{2+}(MGD)_2$, these other $Fe^{2+}(L)_2$ exhibit rate constants for spin trapping ·NO that exceed those found for either nitronyl nitroxides or dendrimer-linked nitronyl nitroxides [11,13]. Of note, the rate constant for $Fe^{2+}(DTCP)_2$ was determined to be ~20 times less than previously reported (Table I). While we currently cannot explain this discrepancy, one possibility is the different kinetic models used in each study.

The ability of $Fe^{2+}(DTCP)_2$, $Fe^{2+}(DTCHP)_2$ and $Fe^{2+}(MSD)_2$ to spin trap ·NO generated by purified NOS I was then investigated. The spin traps, $Fe^{2+}(DTCS)_2$ and $Fe^{2+}(MGD)_2$, were used as standards as these traps have previously shown prominent EPR signals in the presence of activated NOS I [31]. The reaction was commenced by the addition of purified NOS I (300 nM) to a mixture of L-arginine (100 μM), NADPH (1 mM), $CaCl_2$ (2 mM), calmodulin (100 U/ml), and freshly prepared $Fe^{2+}(L)_2$ in phosphate buffer (50 mM, pH 7.4, containing 1 mM EGTA) at room temperature. This high concentration of L-arginine was used to minimize NOS production of $O_2^{\cdot-}$ (e.g. L-arginine $K_m \approx 2$–4 μM, [32]). Under these experimental conditions, the rate of ·NO was found to be ~300 nmole/min/mg protein. This flux of ·NO was chosen to approximate the production of ·NO *in vivo* [33]. As in the case of data shown in Figure 2, a three-lined EPR spectrum for each complex was recorded, denoting formation of $Fe^{2+}(NO)(L)_2$ (Figure 3). EPR spectra for each $Fe^{2+}(NO)(L)_2$ were observed as early as 2 min after the addition of NOS. The spin traps, $Fe^{2+}(DTCP)_2$, $Fe^{2+}(DTCHP)_2$ and $Fe^{2+}(MSD)_2$, gave comparable EPR spectra from NOS I generated ·NO as seen with $Fe^{2+}(DTCS)_2$ and was slightly higher than $Fe^{2+}(MGD)_2$. Exclusion of NADPH from the reaction resulted in no observed EPR spectrum (data not shown), confirming the enzymic formation of ·NO.

For an estimation of the stability of these $Fe^{2+}(NO)(L)_2$ complexes in a relevant biological model, the change in EPR spectra of the various complexes was monitored in the presence of a competent NOS preparation. During the initial phase of the experiment, the EPR spectral peak height of various $Fe^{2+}(NO)(L)_2$ complexes increased, reaching a plateau at approximately 10 min (Figure 4). Thereafter, we observed no significant change in EPR spectral peak height for $Fe^{2+}(NO)(DTCS)_2$, $Fe^{2+}(NO)(MGD)_2$, $Fe^{2+}(NO)(MSD)_2$ and $Fe_{2+}(NO)(DTCP)_2$ for at least 1 h when the experiment was concluded. In contrast, $Fe^{2+}(NO)(DTCHP)_2$ was considerably less stable with a half-life of 15.5 min (Table I) in the presence of NOS I.

Discussion

Several iron–dithiocarbamate chelates, such as $Fe^{2+}(DTCS)_2$, $Fe^{2+}(DETC)_2$, $Fe^{2+}(MGD)_2$, $Fe^{2+}(DTCP)_2$ and $Fe^{2+}(MSD)_2$, have been used as spin traps for ·NO in different experimental paradigms (For review see [34,35]). In this paper, $(NH_4)_2$DTCHP, not studied previously, was also prepared, which when mixed with a $FeSO_4$, formed the complex, $Fe^{2+}(DTCHP)_2$. The spin traps, $Fe^{2+}(DTCS)_2$, $Fe^{2+}(MGD)_2$, $Fe^{2+}(DTCP)_2$, $Fe^{2+}(MSD)_2$ and $Fe^{2+}(DTCHP)_2$, when formed under anaerobic conditions, react with ·NO, forming the corresponding $Fe^{2+}(NO)(DTCS)_2$, $Fe^{2+}(NO)(MGD)_2$, $Fe^{2+}(NO)(DTCP)_2$, $Fe^{2+}(NO)(MSD)_2$ and $Fe^{2+}(NO)(DTCHP)_2$, all of which exhibited the characteristic three-lined EPR spectra.

These spectra were observed using ·NO from either a gaseous solution or generated by NOS I (Figures 2 and 3).

Large k_{app} of $Fe^{2+}(DTCP)_2$ and $Fe^{2+}(MSD)_2$ with ·NO and long lifetimes of $Fe^{2+}(NO)(DTCP)_2$ and $Fe^{2+}(NO)(MSD)_2$ (Table I) suggest that these $Fe^{2+}(L)_2$ are excellent spin traps for ·NO and may, indeed, find applications for detection of ·NO in other biological paradigms including *in vivo*. Although $Fe^{2+}(DTCHP)_2$ has a k_{app} comparable to the other spin traps, the short life time of $Fe^{2+}(NO)(DTCHP)_2$ (Table I) makes the use of $Fe^{2+}(DTCHP)_2$ in *in vivo* applications problematic, however, this spin trap may have promise in many *in vitro* applications. The use of $Fe^{2+}(MSD)_2$ is especially intriguing as this spin trap exhibited a comparable rate constant and similar trapping efficiencies compared to $Fe^{2+}(DTCS)_2$ (Table I and Figure 3). As $Fe^{2+}(DTCS)_2$ is believed to the best spin trap for ·NO, generated from isolated NOSs or ·NO releasing compounds, and has shown promising results in *in vivo* studies [21,31], data obtained with $Fe^{2+}(MSD)_2$ suggest that this spin trap may be an appropriate alternative to $Fe^{2+}(DTCS)_2$ to detect ·NO in a more lipophilic environment. Our data support the preliminary *in vivo* and *ex vivo* experiments of Nakagawa et al. [24] with $Fe^{2+}(MSD)_2$.

Results presented herein suggest that $Fe^{2+}(DTCP)_2$ and $Fe^{2+}(MSD)_2$ are potential spin traps for ·NO with characteristics suitable for many biological applications including those pertinent to the in *vivo, in situ* detection of ·NO.

Acknowledgements

This research was supported in part by a grant from the National Institutes of Health, EB-2034 and R25-GM55036.

References

[1] Furchgott RF. Studies on relaxation of rabbit aorta by sodium nitrite: The basis of the proposal that the acid-activated inhibitory factor from bovine retractor penis is inorganic nitrite and the endothelium-derived relaxing factor is nitric oxide. In: Vanhoutte PM, editor. Vasodilatation: Vascular smooth muscle, peptides, autonomic nerves and endothelium. New York: Raven Press; 1988. p 401–414.

[2] Ignarro LJ, Buga GM, Wood KS, Byrns RE, Chaudhuri G. Endothelium-derived relaxing factor produced and released from artery and vein is nitric oxide. Proc Natl Acad Sci USA 1987;84:9265–9269.

[3] Ignarro LJ, Byrns RE, Wood KS. Biochemical and pharmacological properties of endothelium-derived relaxing factor and its similarity to nitric oxide radical. In: Vanhouttte PM, editor. Vasodilatation: Vascular smooth muscle, peptides, autonomic nerves and endothelium. New York: Raven Press; 1988.

[4] Palmer RM, Ferrige AG, Moncada S. Nitric oxide release accounts for the biological activity of endothelium-derived relaxing factor. Nature 1987;327:524–526.

[5] Moncada S, Palmer RM, Higgs EA. Biosynthesis of nitric oxide from L-arginine. A pathway for the regulation of cell function and communication. Biochem Pharmacol 1989;38:1709–1715.

[6] Stuehr DJ, Nathan CF. Nitric oxide, a macrophage product responsible for cytostasis and respiratory inhibition in tumor target cells. J Exp Med 1989;169:1543–1555.

[7] Bredt DS, Snyder SH. Isolation of nitric oxide synthetase, a calmodulin-requiring enzyme. Proc Natl Acad Sci USA 1990;87:682–685.

[8] Nathan C, Xie Q-W. Nitric oxide synthases: Roles, tolls and controls. Cell 1994;78:915–918.

[9] Lane P, Gross SS. Cell signaling by nitric oxide. Sem Nephrol 1999;19:215–229.

[10] Archer S. Measurement of nitric oxide in biological models. FASEB J 1993;7:349–360.

[11] Akaike T, Yoshida M, Miyamoto Y, Sato K, Kohno M, Sasamoto K, Miyazaki K, Ueda S, Maeda H. Antagonistic action of imidazolineoxyl N-oxides against endothelium-derived relaxing factor/·NO through a radical reaction. Biochemistry 1993;32:827–832.

[12] Joseph J, Kalyanaraman B, Hyde JS. Trapping of nitric oxide by nitronyl nitroxides: An electron spin resonance investigation. Biochem Biophys Res Comm 1993;192:926–934.

[13] Rosen GM, Porasuphatana S, Tsai P, Ambulos NP, Galtsev VE, Ichikawa K, Halpern HJ. Dendrimeric-containing nitronyl nitroxides as spin traps for nitric oxide: Synthesis, kinetic and stability studies. Macromolecules 2003;36:1021–1027.

[14] Vanin AF, Mordvintcev PI, Hauschildt S, Mülsh A. The relationship between Larginine-dependent nitric oxide synthase, nitrite release and dinitrosyl-iron complex formation by activated macrophages. Biochim Biophys Acta 1993;1177:37–42.

[15] Vanin AF, Mordvintcev PI, Kleschev A. Nitric oxide incorporation in animal tissues in vivo. Stud Biophys 1984;102:135–143.

[16] Fujii S, Yoshimura T, Kamada H. Nitric oxide trapping efficiencies of water-soluble iron(III) complexes with dithiocarbamate derivatives. Chem Lett 1996;:785–786.

[17] Shinobu LA, Jones SG, Jones MM. Sodium *N*-methyl-D-glucamine dithiocarbamate and cadmium intoxication. Acta Pharmacol Toxicol 1984;54:189–194.

[18] Komarov AM, Lai C-S. Detection of nitric oxide production in mice by spin-trapping electron paramagnetic resonance spectroscopy. Biochim Biophys Acta 1995;1272:29–36.

[19] Yoshimura T, Fujii S, Yokoyama H, Kamada H. *In vivo* electron paramagnetic resonance imaging of NO-bound iron complex in a rat head. Chem Lett 1995;:309–310.

[20] Yoshimura T, Yokoyama H, Fujii S, Takayama F, Oikawa K, Kamada H. *In vivo* EPR detection and imaging of endogenous nitric oxide in lipopolysaccharide-treated mice. Nature Biotech. 1996;14:992–994.

[21] Pou S, Tsai P, Porasuphatana S, Rosen GM. Spin trapping of nitric oxide by ferrochelates: Kinetic and *in vivo* pharmacokinetic studies. Biochim Biophys Acta 1999;1427:216–226.

[22] Kotake Y. Continuous and quantitative monitoring of rate of cellular nitric oxide generation. Methods Enzymol 1996; 268:222–229.

[23] Lai C-S, Komarov AM. Spin trapping of nitric oxide produced *in vivo* in septic-shock mice. FEBS Lett 1994;345:120–124.

[24] Nakagawa H, Ikota N, Ozawa T, Masumizu T, Kohno M. Spin trapping for nitric oxide produced in LPS-treated mouse using various new dithiocarbamate iron complexes having substituted proline and serine moiety. Biochem Mol Bio Int 1998;45:1129–1138.

[25] Paschenko SV, Khramtsov VV, Skatchkov MP, Plyusnin VF, Bassenge E. EPR and laser flash photolysis studies of the reaction of nitric oxide with water soluble NO trap Fe(II)-proline dithiocarbamate complex. Biochem Biophys Res Comm 1996;225:557–584.

[26] Roman LJ, Sheta EA, Martasek P, Gross SS, Liu Q, Masters BSS. High-level expression of functional rat neuronal nitric oxide synthase in *Escherichia coli*. Proc Natl Acad Sci USA 1995;92:8428–8432.

[27] Fujii H, Koscielniak J, Berliner LJ. Determination and characterization of nitric oxide generation in mice by *in vivo* L-Band EPR spectroscopy. Magnetic Reson Med 1997;38:565–568.

[28] Hevel JM, Marletta MA. Nitric-oxide synthase assay. Methods Enzymol 1994;233:250–258.

[29] Mordvintcev P, Mulsch A, Busse R, Vanin A. On-line detection of nitric oxide formation in liquid aqueous phase by electron paramagnetic resonance spectroscopy. Anal Biochem 1991;199:142–146.

[30] Doyle MP, Hoekstra JW. Oxidation of nitrogen oxides by bound dioxygen in hemoproteins. J Inorg Biochem 1981;14:351–358.

[31] Porasuphatana S, Weaver J, Budzichowski TA, Tsai P, Rosen GM. Differential effect of buffer on the spin trapping of nitric oxide by iron chelates. Anal Biochem 2001; 298:50–56.

[32] Nathan C. Nitric oxide as a secretory product of mammalian cells. FASEB J 1992;6:3051–3064.

[33] Malinski T, Kapturczak M, Dayharsh J, Bohr D. Nitric oxide synthase activity in genetic hypertension. Biochem Biophys Res Commun 1993;194:960–965.

[34] Berliner LJ, Fujii H. *In vivo* spin trapping of nitric oxide. Antioxid Redox Signal 2004;6:649–656.

[35] Yoshimura T, Kotake Y. Spin trapping of nitric oxide with iron–dithiocarbamate complex: Chemistry and biology. Antioxid Redox Signal 2004;6:639–647.

[36] Kao JPY, Rosen GM. Esterase-assisted accumulation of 3-carboxy-2,2,5,5-tetramethyl-1-pyrrolidinyloxyl into lymphocytes. Org Biomol Chem 2004;2:99–102.